Drug-loaded, bivalent-bottle-brush polymers by graft-through ROMP

Jeremiah A. Johnson, **Ying Y. Lu**, **Alan O. Burts**, **Yan Xia**, **Alec C. Durrell**, **David A. Tirrell**, and **Robert H. Grubbs**
Division of Chemistry and Chemical Engineering, California Institute of Technology, 1200 E. California Blvd., Pasadena, California 91125

Abstract

Graft-through ring-opening metathesis polymerization (ROMP) using ruthenium *N*-heterocyclic carbene catalysts has enabled the synthesis of bottle-brush polymers with unprecedented ease and control. Here we report the first bivalent-brush polymers; these materials were prepared by graft-through ROMP of drug-loaded polyethylene-glycol (PEG) based macromonomers (MMs). Anticancer drugs doxorubicin (**DOX**) and camptothecin (**CT**) were attached to a norbornene-alkyne-PEG MM via a photocleavable linker. ROMP of either or both drug-loaded MMs generated brush homo- and co-polymers with low polydispersities and defined molecular weights. Release of free **DOX** and **CT** from these materials was initiated by exposure to 365 nm light. All of the **CT** and **DOX** polymers were at least 10-fold more toxic to human cancer cells after photoinitiated drug release while a copolymer carrying both **CT** and **DOX** displayed 30-fold increased toxicity upon irradiation. Graft-through ROMP of drug-loaded macromonomers provides a general method for the systematic study of structure-function relationships for stimuli-responsive polymers in biological systems.

Introduction

Recent advances in catalysis and polymer synthesis have allowed the preparation of new materials with unprecedented functional and structural diversity and blurred the line between small-molecule and polymer synthesis.[1,2] Ring-opening metathesis polymerization (ROMP) using fast-initiating ruthenium catalysts (e.g. **1**, Figure 1) is particularly suited for the synthesis of diverse side-chain functional polymers with controllable molecular weights (M_n) and low polydispersities (PDI).[3–6]

Discrete bottle-brush polymers (brush polymers) are typically comprised of a linear polymer backbone connected at each monomer unit to a polymeric sidechain. Brush polymers with two polymer side-chains attached to each monomer unit of a polymer backbone (centipede-brushes) have been reported; these materials can possess disparate polymer domains within the same polymer structure.[7–9] Synthetic approaches to all types of brush polymers fall into "graft-to," "graft-from," or "graft-through" categories; each approach has advantages and disadvantages.[10] For example, graft-to and graft-from strategies, whereby linear polymers are coupled to the backbone of a linear polymer or are grown from the backbone of a linear macroinitiator respectively, are suited to most polymerization methods but suffer from sterically limited grafting densities for even the most efficient coupling and polymerization

reactions.[11−20] The alternative graft-through approach, which involves polymerization of well-defined monofunctional macromonomers (MMs), ensures quantitative grafting density but requires a polymerization method capable of propagation under conditions of very low monomer concentration and high steric hindrance.[21−26] Thus, most brush polymers made by graft-through approaches have significant amounts of MM impurities due to incomplete conversion; few examples of functional systems of high degree of polymerization (DP_n) have been reported.[27,28]

Recently, our group and others have shown the utility of ROMP using catalyst **1** for the graft-through polymerization of a variety of norbornene-terminated MMs to yield brush homo- and co-polymers that have high DP_ns and low PDIs.[27−31] These studies have set a benchmark for efficiency in brush polymer synthesis and led us to explore the application of graft-through ROMP to the synthesis of novel bivalent-brush polymers (Figure 1) with one branch comprised of a hydrophilic solubilising polymer (polyethylene glycol) and the other a drug molecule covalently attached through a degradable linker. Brush polymers and other branched polymeric architectures (dendrimers, hyperbranched polymers, dendronized polymers, etc…) possess features, such as multivalency and nanoscopic size, which make them attractive for *in vivo* drug delivery applications.[32−34] Branched structures of sufficient size display extended *in vivo* circulation times in comparison to their linear analogues - an advantageous feature for passive tumor targeting via the enhanced permeation and retention effect (EPR effect).[35,36] Dendrimers are the most extensively studied branched polymers in this regard; their monodisperse, globular structures resemble those of proteins and render them attractive for biological applications.[37,38] Despite the promise of dendrimers, synthetic challenges limit their utility in therapeutic applications. It is difficult to prepare dendrimers larger than ~10 nm due to the steric hindrance which must be overcome when functionalizing the periphery of a high-generation dendritic structure. To overcome this limitation, the Fréchet group has appended linear polyethylene glycol (PEG) chains to dendrimers to increase their size, water solubility, and biocompatibility while retaining their inherent multivalency.[39−41] These "PEGylated" dendrimers have proven remarkably effective for treatment of cancer in mice via controlled delivery of doxorubicin (**DOX**)[39] and camptothecin (**CT**).[41] Though large polymers may be preferable in certain applications, several reports suggest that non-degradable polymers for drug delivery applications must be no larger than ~10 nm to ensure complete renal clearance.[35,42] A synthetic approach capable of rapidly generating branched polymeric structures of easily variable sizes is highly desirable.

Here we introduce a new bivalent-brush polymer structure for use in chemotherapy delivery. Figure 1 depicts a schematic of our design; a water-soluble PEG sidechain and a drug molecule are attached to a polynorbornene backbone via a branch point. The drug is attached via a degradable linker that allows controlled release in response to an appropriate stimulus. We expect the PEG chains to extend into solution effectively shielding the hydrophobic drug +polynorbornene core; the structure resembles that of a unimolecular micelle. We reasoned that these bivalent-brush polymers might exhibit similar drug-delivery attributes when compared to PEGylated dendrimers but may be easier to synthesize, especially over a wide range of nanoscale sizes and with greater functional diversity, using graft-through ROMP of a PEGylated-norbornene MM. Here we demonstrate the power of this approach for the preparation of water-soluble polynorbornene-*g*-PEG brush polymers and copolymers that have **DOX** and **CT** covalently bound near the core through a photocleavable linker. Brief ultraviolet (UV, 365 nm) irradiation of these brush polymers releases the respective drug molecules in unmodified form; we demonstrate the utility of these systems for photoregulated chemotherapy delivery in human cancer cell culture.

Materials and methods

All reagents and solvents were purchased from Aldrich or VWR chemical companies and were used as supplied unless otherwise noted. Ruthenium catalyst **1**,[43] 3-azidopropyl-1-amine (note: care must be taken when working with small-molecule, < 6 carbons per azide, azides. In this work, 3-azidopropyl-1-amine is used as a ~1 M solution in toluene and never isolated),[44] and 3-(*tert*-butyldimethylsilyloxymethyl)-2-nitrobenzoic acid **8**[45] were prepared according to literature procedures. Degassed dichloromethane (DCM), tetrahydrofuran (THF), and dimethyl sulfoxide (DMSO) solvents were passed through solvent purification columns prior to use.[46] Doxorubicin hydrochloride (**DOX**-HCl) was purchased from Axxora LLC.

Gel permeation chromatography (GPC) was performed using two I-series Mixed Bed Low MW ViscoGel columns (Viscotek) connected in series with a DAWN EOS multiangle laser light scattering (MALLS) detector (Wyatt Technology) and an Optilab DSP differential refractometer (Wyatt Technology). Experiments were performed at room temperature using 0.2 M LiBr in *N,N*-dimethylformamide (DMF) eluant at a flow rate of 1 mL / min. Molecular weights were calculated from *dn/dc* values that were obtained assuming 100% mass elution from the columns. Dynamic light scattering (DLS) measurements were made at room temperature using a Brookhaven ZetaPALS DLS instrument. Samples were dissolved in nanopure water at a concentration of ~1 mg / mL. A fresh, clean, polystyrene cuvette was washed with compressed air to remove dust. The sample solution was passed through a 0.4 µm Teflon syringe filter directly into the cuvette; the cuvette was capped and placed in the DLS for particle sizing. At least 3 measurements were made per sample and average hydrodynamic diameters were calculated by fitting the DLS correlation function using the CONTIN routine (ISDA software package from Brookhaven instruments). Nuclear magnetic resonance (NMR) experiments were performed on either a Mercury 300 MHz spectrometer, an INOVA 500 MHz spectrometer, or an INOVA 600 MHz spectrometer. Varian VNMRJ and MestReNove NMR 5.3.2 software were used to obtain and analyze the NMR spectra, respectively. Analytical high-performance liquid chromatography mass spectrometry (HPLC-MS or LC-MS) data was obtained using an Agilent 1100 series HPLC system equipped with a variable wavelength ultraviolet-visible (UV-Vis) detector and an Agilent 1100 VL LC/MSD mass spectrometer. Separation was achieved using a 9.4×50 mm Agilent Zorbax XDB-C18 column with mobile phase gradients of 0.1% acetic acid in water and acetonitrile. Experiments were performed at room temperature with a flow rate of 1.0 mL / min. Preparatory HPLC was performed on an Agilent 1100 series HPLC system with an Agilent 1200 series automated fraction collector and an 1100 series variable wavelength detector. Separation was achieved using a 9.4×250 mm Agilent Eclipse XDB-C18 column with 0.1% acetic acid in water and acetonitrile mobile phase. Experiments were performed at room temperature with a flow rate of 5 mL / min. High-resolution mass spectrometry data was obtained on an Agilent 6200 series accurate-mass time-of-flight (TOF) LC/MS. Matrix assisted laser desorption ionization mass spectrometry (MALDI) measurements were performed by the California Institute of Technology mass spectrometry facility using a Voyager De_Pro TOF mass spectrometer (Applied Biosystems) fitted with a 355 nm YAG laser from Blue Ion Technologies. In a typical experiment, 1.0 mg of polymer sample was dissolved in 100 µL of THF and diluted 10-fold with the MALDI matrix, dithranol (10 mg / mL in THF). To each sample was added 0.1 µL of saturated NaI in ethanol and 0.35 µL of the sample-matrix mixture was spotted on a MALDI plate for analysis. The Voyager De_Pro was operated in linear mode with an accelerating voltage of 20,000 V, grid voltage of 95.2%, guide wire 0.03%, extraction delay time 250 ns, acquisition mass range 800–5000 Da, and laser rep rate 20 Hz. The instrument was calibrated externally using a Sequazyme Mass Standard Kit supplied by Applied Biosystems. Brush polymer purification was performed by centrifugal filtration through 30 kDa molecular-weight cut off (MWCO)

Amicon Ultra-15 centrifugal filter units (Millipore Inc.). Photolysis experiments were performed using a Multiple Ray Lamp (UVP) fitted with an 8 W, longwave, filtered blacklight bulb (365 nm). Sample vials were placed as close as possible to the light source and irradiated for the desired time before analysis by LC-MS.

Norbornene-hexanol (2)

A solution of 6-amino-1-hexanol (3.0 g, 25.6 mmol) and *cis*-5-norbornene-*exo*-2,3,-dicarboxylic anhydride (4.0 g, 24.4 mmol) in toluene (50 mL) was added to a dried, 150 mL round-bottom flask fitted with a Dean-Stark trap and placed in an oil bath preset to 140 °C for 24 h while stirring. The reaction mixture was transferred to a silica gel column primed using 10% ethyl acetate in hexanes (10% EtOAc/hexane). A 300 mL portion of 10% EtOAc/hexanes was flushed through the column before elution of the product using 50% EtOAc/hexanes (TLC $R_f = 0.3$, 50% EtOAc/hexanes, $KMnO_4$ stain). Removal of solvent by rotary evaporation yielded 6.0 g of **2** as a colorless oil (94%). ^{1}H NMR (300 MHz, $CDCl_3$): δ 6.00 (s, 2H), 3.26 (t, *J* = 6.4 Hz, 2H), 3.13 (t, *J* = 7.3, 2H), 2.93 (s, 2 H), 2.38 (s, 2H), 1.31 – 1.15 (m, 5H), 1.14 – 0.95 (m, 4H), 0.92 (t, *J* = 7.4 Hz, 1H); ^{13}C NMR (300 MHz, $CDCl_3$): δ 177.9, 137.5, 61.8, 47.5, 44.8, 42.4, 38.3, 32.2, 27.4, 26.4, 25.0; TOF HRMS calcd. for $C_{15}H_{22}NO_3$ [M+H]$^+$ 264.1600, found 264.1612.

Norbornene-aldehyde (3)

A three-neck round bottom flask containing a stir bar was equipped with a vacuum adaptor and two 150 mL addition funnels each capped with a rubber septum. The flask was flame dried under vacuum, cooled to room temperature, and backfilled with argon. A positive argon pressure (using a mercury bubbler) was maintained through the course of the reaction. DCM (58 mL) was added to the flask via cannula followed by oxalyl chloride (3.21 mL, 37.36 mmol). The solution was cooled to −76 °C using an acetone/dry ice bath. One of the addition funnels was charged with DCM (7.3 mL) and DMSO (5.31 mL, 74.72 mmol) while alcohol **3** (6.60 g, 24.90 mmol) dissolved in DCM (43 mL) was added to the other. The DMSO/DCM solution was added dropwise to the flask containing oxalyl chloride over 15 min while stirring. After the addition, the solution was stirred for 15 min at −76 °C. The solution of **3** in DCM was then added dropwise over 20 min while stirring. The addition funnel was washed twice with 5 mL of DCM and the reaction mixture was stirred for 30 min at −76 °C. Triethylamine (20.83 mL, 149.4 mmol) and DCM (3.7 mL) were combined in the washed addition funnel that previously held **3** and this solution was added dropwise over 15 min to the flask during which time a thick white precipitate formed. After the addition the mixture was stirred for 10 min before warming to room temperature and transferring to a separatory funnel. The mixture was washed twice with 50 mL of 1 M HCl and once with brine, dried over Na_2SO_4 and concentrated on a rotary evaporator. The crude product was purified by silica gel column chromatography (30% EtOAc/hexanes, TLC $R_f = 0.25$, stain with anisaldehyde solution) to yield **3** (5.83 g, 89%) as a colorless oil. ^{1}H NMR (300 MHz, $CDCl_3$): δ 9.52 (s, 1H), 6.08 (s, 2H) 3.23 (t, *J* = 7.3 Hz, 2H), 3.02 (s, 2H), 2.46 (s, 2H), 2.22 (td, *J* = 7.2, 1.4 Hz, 2H), 1.52 – 1.22 (m, 5H), 1.21 – 1.05 (m, 2H), 0.99 (d, *J* = 9.8 Hz, 1H); ^{13}C NMR (300 MHz, $CDCl_3$): δ 202.0, 177.7, 137.6, 47.6, 44.9, 43.3, 42.5, 38.1, 27.3, 26.2, 21.3; TOF HRMS calcd. for $C_{15}H_{19}NO_3$ [M+H]$^+$ 262.1443, found 262.1438.

Norbornene-alkyne-amine (4)

Aldehyde **3** (1.0 g, 3.83 mmol) and propargyl amine (258 μL, 4.0 mmol) were dissolved in methanol (10 mL) in a round-bottom flask. The mixture was stirred at room temperature under argon atmosphere for 30 min to form an imine intermediate (reaction monitored by TOF-LC/MS, calcd. for imine $C_{18}H_{22}N_2O_2$ [M+H]$^+$: 299.1754, found: 299.1856). The reaction mixture was cooled to 0 °C using an ice bath; $NaBH_4$ (232 mg, 6.13 mmol) was carefully added. The ice bath was removed and the mixture was stirred for 3 min before

quenching with 100 mL of saturated NaHCO$_{3(aq.)}$. The mixture was transferred to a separatory funnel and washed five times with DCM (100 mL). The organic fractions were combined and dried over Na$_2$SO$_4$, filtered, and concentrated on a rotary evaporator. The resulting oil was purified by silica gel chromatography (2% MeOH/CH$_2$Cl$_2$, TLC R$_f$ = 0.2, stain with ninhydrin solution) to yield **4** as a colorless oil (836 mg, 73%). ^{1}H NMR (300 MHz, CDCl$_3$): δ 6.18 (s, 2H), 3.33 (t, J = 7.3 Hz, 2H), 3.29 (d, J = 2.4 Hz, 2H), 3.14 (s, 2H), 2.62 – 2.46 (m, 4H), 2.12 (t, J = 2.4 Hz, 1H), 1.53 – 1.30 (m, 5H), 1.30 – 1.14 (m, 5H), 1.10 (d, J = 9.8 Hz, 1H); ^{13}C NMR (300 MHz, CDCl$_3$): δ 177.9, 137.7, 82.2, 71.2, 48.3, 47.7, 45.0, 42.6, 38.5, 38.0, 29.5, 27.6, 26.7, 26.6; TOF HRMS calcd. for C$_{18}$H$_{24}$N$_2$O$_2$ [M+H]$^+$ 301.1911, found 301.1951.

Norbornene-acid-alkyne (5)

Succinic anhydride (134 mg, 1.34 mmol) was combined with amine **4** (382 mg, 1.28 mmol) in DCM (13 mL) and the resulting solution was stirred for 1 h at room temperature before transferring to a silica gel column. Elution with 60% EtOAc/hexanes (TLC R$_f$ = 0.2, stain with bromocresol green solution) gave the purified acid **5** (364 mg, 71%) as a mixture of amide rotamers after concentration on a rotary evaporator. ^{1}H NMR (300 MHz, CDCl$_3$): δ 9.25 (b, 1H), 6.24 (s, 2H), 4.15 (d, J = 2.4 Hz, 1.2H), 4.01 (d, J = 2.3 Hz, 0.8H), 3.50 – 3.31 (m, 4H), 3.22 (s, 2H), 2.82 – 2.50 (m, 6H), 2.29 (t, J = 2.3 Hz, 0.3H), 2.17 (t, J = 2.5 Hz, 0.7H), 1.68 – 1.40 (m, 5H), 1.39 – 1.21 (m, 5H), 1.16 (d, J = 9.8 Hz, 1H); ^{13}C NMR (300 MHz, CDCl$_3$): δ 178.2, 177.0, 171.6, 171.1, 137.8, 78.9, 78.4, 72.8, 71.8, 47.8, 47.1, 46.6, 45.1, 42.7, 38.5, 38.4, 37.5, 34.6, 29.4, 29.3, 28.1, 28.0, 27.9, 27.5, 27.2, 26.5, 26.2; TOF HRMS calcd. for C$_{22}$H$_{27}$N$_2$O$_5$ [M−H]$^-$ 399.1920, found 399.1941.

Norbornene-alkyne-*N*-hydroxysuccinimidyl (NHS)-ester (6)

DCM (10 mL) was added to a flask containing *N*-(3-dimethylaminopropyl)-*N′*-ethylcarbodiimide hydrochloride (EDCI, 262 mg, 1.36 mmol), *N*-hydroxysuccinimide (157 mg, 1.36 mmol), 4-(dimethylamino)pyridine (DMAP, 11.1 mg, 0.091 mmol), and **5** (364 mg, 0.91 mmol). The resulting solution was stirred under argon at room temperature for 20 h. The mixture was transferred to a silica gel column. Elution with 70% EtOAc/hexanes (TLC R$_f$ = 0.2, stain with anisaldehyde solution and/or visualize under UV light) gave norbornene **6** (339 mg, 75%) after concentration on a rotary evaporator. ^{1}H NMR (300 MHz, CDCl$_3$): δ 6.23 (s, 2H), 4.16 (d, J = 2.4 Hz, 1.2 H), 3.98 (d, J = 2.2 Hz, 0.8 H), 3.49 – 3.26 (m, 4H), 6.23 (s, 2H), 2.95 (t, J = 6.9 Hz, 2H), 2.79 (s, 4H), 2.70 (t, J = 6.9 Hz, 2H), 2.62 (s, 2H), 2.29 (t, J = 2.4 Hz, 0.3H), 2.17 (t, J = 2.5 Hz, 0.7H), 1.68-1.40 (m, 5H), 1.39 – 1.20 (m, 5H); ^{13}C NMR (300 MHz, CDCl$_3$): δ 178.0, 169.6, 169.3, 169.0, 168.4, 137.8, 78.9, 78.4, 77.5, 76.7, 72.9, 71.8, 47.7, 46.9, 46.6, 45.1, 42.7, 38.5, 38.3, 37.4, 34.4, 28.1, 28.0, 27.8, 27.6, 27.5, 27.3, 26.5, 26.2, 25.6; TOF HRMS calcd. for C$_{26}$H$_{32}$N$_3$O$_7$ [M+H]$^+$ 498.2241, found 498.2203.

Norbornene-alkyne-PEG(3000) macromonomer (7)

O-(2-Aminoethyl)polyethylene glycol (100 mg, 33.3 µmol) and **6** (17.4 mg, 35 µmol) were dissolved in anhydrous DMF (1 mL) and the resulting solution was stirred at room temperature for 4 h. The reaction mixture was added dropwise to diethyl ether (20 mL) to precipitate **7** as a white solid which was collected by centrifugation and decanting of the ether before redissolving in DCM (1 mL). This process of precipitation, centrifugation, and re-dissolving was repeated five times. On the fifth iteration, the precipitate was dried under vacuum to afford macromonomer **7** as a white powder (78.1 mg, 69%). GPC (0.2 M LiBr in DMF) 3,300 Da, PDI 1.10. MALDI mass spectrum and NMR are shown in supporting information (Figures S1–S3).

N-(3-azidopropyl)-3-(*tert*-butyldimethylsilyloxymethyl)-2-nitrobenzamide (9)

EDC (92.4 mg, 0.48 mmol) was added to a suspension of acid **8** (100 mg, 0.32 mmol) and DMAP (3.9 mg, 0.032 mmol) in DCM (4.0 mL). The suspension became a clear solution within 2 min indicating formation of a soluble acylisourea intermediate. At this time, 3-azidopropyl-1-amine (1.0 M in toluene, 482 μL, 0.48 mmol) was added dropwise to the reaction mixture. The resulting solution was stirred overnight at room temperature under an argon atmosphere. The reaction mixture was diluted with 100 mL EtOAc and washed three times with 1.0 M HCl (50 mL), three times with sat. NaHCO$_3$ (50 mL), and once with brine (50 mL). The organic layer was then dried over MgSO$_4$, filtered, and concentrated on a rotary evaporator. The resulting white solid was passed through a silica plug using 50% EtOAc/hexanes and evaporated to dryness to give **9** (101 mg, 80%) as a white crystalline solid (128 mg, 80%). ^{1}H NMR (300 MHz, CDCl$_3$): δ 7.75 (d, *J* = 6.4 Hz, 1H), 7.52 (t, *J* = 7.7 Hz, 1H), 7.41 (d, *J* = 6.2 Hz, 1H), 6.46 (b, 1H), 4.78 (s, 2H), 3.65 – 3.15 (m, 4H), 1.84 (p, *J* = 6.6 Hz, 2H), 0.92 (s, 9H), 0.09 (s, 6H); ^{13}C NMR (300 MHz, CDCl$_3$): δ 165.8, 146.4, 135.4, 131.2, 130.7, 129.9, 126.5, 60.8, 49.3, 37.8, 28.4, 25.0, 18.3, 5.6; TOF HRMS calcd. for C$_{17}$H$_{28}$N$_5$O$_4$Si [M+H]$^+$ 394.1911, found 394.1900.

N-(3-azidopropyl)-3-(hydroxymethyl)-2-nitrobenzamide (10)

Compound **9** (101 mg, 0.26 mmol) was dissolved in tetrahydrofuran (3 mL) in a round bottom flask which was subsequently cooled to 0 °C. Tetrabutylammonium fluoride (1.0 M in THF, 0.385 mL, 0.39 mmol) was added dropwise and the mixture was stirred for 15 min. The solution was diluted with EtOAc (50 mL) and washed three times with 1.0 M HCl (25 mL) and once with brine (50 mL). The organic layer was dried over MgSO$_4$, filtered, and passed through a silica plug to give pure **10** (56 mg, 78%) as a white solid. ^{1}H NMR (300 MHz, acetone): δ 7.98 (b, 1H), 7.82 (d, *J* = 4.6 Hz, 1H), 7.69 – 7.56 (m, 2H), 4.71 (s, 2H), 3.63 – 3.28 (m, 4H), 1.88 (p, *J* = 6.8 Hz, 2H); ^{13}C NMR (300 MHz, acetone): δ 205.4, 165.2, 135.3, 130.8, 130.1, 126.9, 59.4, 48.8, 36.9; TOF HRMS calcd. for C$_{11}$H$_{13}$N$_5$O$_4$ [M +H]$^+$ 280.1046, found 280.1067.

CT-NBOC-N3

The following reaction was a modified literature procedure for the preparation of 20-*O*-acylcamptothecins.[47] (*S*)-(+)-Camptothecin (**CT**, 62.7 mg, 0.18 mmol) and DMAP (70.1 mg, 0.57 mmol) were suspended in DCM (5 mL) under argon atmosphere. Triphosgene (19.6 mg, 0.066 mmol) was added and the mixture was stirred for 30 min at RT. Alcohol **10** (55.2 mg, 0.2 mmol, in 2 mL THF) was added dropwise via a rubber septum using a gastight syringe. The reaction was stirred overnight during which time a white precipitate formed. The reaction mixture was diluted with EtOAc (100 mL) and washed once with water (50 mL), twice with 1.0 M HCl (25 mL), and once with brine (50 mL). The organic layer was dried over MgSO$_4$, filtered, and concentrated on a rotary evaporator. The solid residue was purified by column chromatography (100% EtOAc, TLC R$_f$ = 0.2, visualize under UV light) to give **CT-NBOC-N$_3$** as a white solid (106 mg, 90%). ^{1}H NMR (600 MHz, CDCl$_3$): δ 8.41 (s, 1H), 8.26 (d, *J* = 8.6 Hz, 1H), 7.95 (d, *J* = 7.8 Hz, 1H), 7.86 (ddd, *J* = 8.4, 6.9, 1.4 Hz, 1H), 7.72 – 7.68 (m, 2H), 7.56 (t, *J* = 7.7 Hz, 1H), 7.43 (dd, *J* = 7.6, 1.3 Hz, 1H), 7.34 (s, 1H), 6.33 (t, *J* = 5.8 Hz, 1H), 5.59 (d, *J* = 17.1 Hz, 1H), 5.34 (d, *J* = 17.1 Hz, 1H), 5.32 – 5.19 (m, 4H), 3.46 (q, *J* = 6.5 Hz, 2H), 3.42 (t, *J* = 6.5 Hz, 2H), 2.27 (dt, *J* = 14.9, 7.5 Hz, 1H), 2.21 – 2.11 (m, 1H), 1.85 (p, *J* = 6.5 Hz, 2H), 1.01 (t, *J* = 7.5 Hz, 3H); ^{13}C NMR (300 MHz, CDCl$_3$): δ 167.1, 165.5, 157.2, 153.0, 151.9, 148.5, 146.9, 146.3, 145.4, 131.9, 131.8, 131.5, 131.0, 130.4, 129.5, 129.3, 128.5, 128.3, 128.2, 128.1, 120.3, 96.1, 78.5, 67.0, 65.3, 50.0, 49.2, 45.0, 37.8, 31.8, 28.4, 7.6; TOF HRMS calcd. for C$_{32}$H$_{28}$N$_7$O$_9$ [M+H]$^+$ 654.1949, found 654.2010.

DOX-NBOC-N3

A suspension of **10** (45 mg, 0.16 mmol) in THF (2 mL) and triethylamine (25 µL, 0.18 mmol) was treated with 4-nitrophenyl chloroformate (35 mg, 0.18 mmol). TLC and ^{1}H NMR confirmed complete conversion to carbonate **11** within 15 min. The reaction mixture was transferred to a short silica gel column and eluted with 70% EtOAc. UV active fractions with $R_f = 0.4$ were combined and dried on a rotary evaporator. The resulting white solid, **11** (40 mg, 90 µmol), was immediately dissolved in anhydrous DMF (1 mL). **DOX**-HCl (53 mg, 91 µmol) and anhydrous *N,N*-diisopropylethylamine (DIPEA, 17 µL, 99 µmol) were added and the resulting solution was stirred overnight at room temperature. The reaction mixture was diluted with 50 mL EtOAc and washed twice with 0.1 M HCl (20 mL), once with H_2O (20 mL), and once with brine (20 mL) before drying over magnesium sulfate, filtration, and concentration on a rotary evaporator. The resulting red solid was purified by column chromatography. The column was eluted first with 3% $MeOH/CH_2Cl_2$ and then with 5% $MeOH/CH_2Cl_2$ to give **DOX-NBOC-N3** as a red solid (73 mg, 95%). ^{1}H NMR (600 MHz, DMSO-d_6): δ 8.77 (t, *J* = 5.6 Hz, 1H), 7.96 - 7.87 (m, 2H), 7.67 - 7.61 (m, 3H), 7.57 (dd, *J* = 6.9, 2.1 Hz, 1H), 7.00 (d, *J* = 8.0 Hz, 1H), 5.42 (s, 1H), 5.20 (s, 1H), 5.01 (dd, *J* = 37.8, 13.7 Hz, 2H), 4.92 (m, 1H), 4.81 (t, *J* = 6.0 Hz, 1H), 4.69 (d, J = 5.7 Hz, 1H), 4.54 (d, J = 6.0 Hz, 2H), 4.14 - 4.09 (m, 1H), 3.98 (s, 3H), 3.71 - 3.60 (m, 1H), 3.42 - 3.39 (m, 1H), 3.38 - 3.35 (m, 2H), 3.24 - 3.19 (m, 2H), 2.96 (q, *J* = 18.3 Hz, 2H), 2.12 (dt, *J* = 14.5, 9.0 Hz, 2H), 1.83 (dd, *J* = 12.8, 9.2 Hz, 1H), 1.69 (p, *J* = 6.7 Hz, 2H), 1.09 (d, *J* = 6.5 Hz, 4H); ^{13}C NMR (500 MHz, CD_2Cl_2): δ 213.1, 186.1, 164.5, 160.4, 155.3, 154.7, 154.0, 146.7, 135.0, 134.6, 132.8, 132.7, 130.6, 130.5, 130.4, 130.1, 126.7, 120.0, 118.7, 117.9, 110.8, 110.7, 99.8, 75.9, 68.7, 68.6, 66.6, 64.7, 61.2, 55.8, 48.6, 46.4, 37.0, 34.8, 33.2, 28.9, 27.7, 15.8; TOF HRMS calcd. for $C_{39}H_{40}N_6O_{16}$ [M−H]$^−$ 847.2423, found 847.2418.

General macromonomer synthesis by copper-catalyzed azide-alkyne cycloaddition (CuAAC) click chemistry

Drug azide, **CT-NBOC-N$_3$** or **DOX-NBOC-N$_3$**, (1.01 equiv. to alkyne) was combined with norbornene-PEG-alkyne **3** (100 mg, 29.4 µmol) in a 2 mL HPLC vial and THF (0.5 mL) was added. A spatula tip of sodium ascorbate was added followed by a 1.0 M solution of $CuSO_4$ in H_2O (88 µL, 3 equiv. to alkyne). The mixture was flushed with argon, sealed with a septum, and stirred until completion (as monitored by LC-MS) which was typically ~1 h. After the required time, the drug-loaded macromonomer was purified by preparative HPLC (linear gradient of 95:5 water-0.1% AcOH:MeCN to 5:95 water-0.1% AcOH-MeCN over 12 min). The fractions containing pure MM were combined and concentrated on a rotary evaporator. The resulting residue was dissolved in DCM, dried over Na_2SO_4, filtered, and dried under vacuum to give pure macromonomer **CT-MM** or **DOX-MM** (typical yield ~75 mg, ~70%). MALDI and ^{1}H NMR spectra are shown in supporting information (Figures S4–S7).

General ROMP polymerization

Macromonomer **DOX-MM** or **CT-MM** (20 mg, ~5 µmol), or a combination of the two, was added to a 2 mL vial containing a stir bar. The vial was capped with a septum and placed under vacuum for 5 min and then purged with argon. DCM was added followed by a freshly prepared solution of catalyst **1** in DCM (1 mg **1** / mL DCM, amount added to give the desired MM:**1**) such that the total concentration of MM was 0.05 M. The mixture was stirred at room temperature under argon for 90 min after which time the reaction became noticeably viscous. One drop of ethyl vinyl ether was added to quench the polymerization and the vial was placed under vacuum to remove volatiles. The resulting polymer film was dissolved in deionized water (15 mL) and transferred to a centrifugal filter tube (30 kDa MWCO). The tube was spun at 4000 rpm until all of the solvent had passed through the filter except for ~1 mL (typically ~45 min). More water was added (14 mL) and this process was repeated at

least 5 times to remove any remaining MM. After the last centrifugation, the 1 mL solution of brush polymer in water was transferred to a weighed glass vial and lyophilized to dryness. Typical yields after purification were ~15 mg (75%). Representative ^{1}H NMR spectra are shown in supporting information (Figures S8 and S9).

LC-MS methods

Two methods were used for analytical LC-MS experiments; acetonitrile (MeCN) percentage was varied. Method A was a linear gradient of 5% MeCN to 95% MeCN over 5 min followed by a 2 minute hold at 95% MeCN to flush the column. Method B began at 5% MeCN and ran to 70% MeCN linearly over 5 min followed by a 2 min flush at 95% MeCN. Method A was used for the **DOX** loaded polymers (**pDOX02** and the copolymer) and method B for **pCT03**. The concentration of **CT** and/or **DOX** in photolyzed samples was estimated from free **CT** and **DOX** calibration curves, respectively. The calibration curves were generated as follows. A 1 mM solution of **CT** in DMSO was serially diluted with DMSO to generate 100 µM, 10 µM, and 1 µM solutions. In a similar fashion, a 1 mM solution of **DOX**-HCl in water was serially diluted with water to generate 50 µM, 10 µM, and 1 µM solutions. Each of these samples was analyzed by LC-MS with wavelength detection set at 368 nm and 500 nm for **CT** and **DOX** respectively. Method A was used in both cases. The area under the absorbance curve for each run was calculated and plotted against the concentration of drug (Figure S10). Linear fitting of the resulting calibration curve gave an extinction coefficient that was used to estimate the concentration of drug released in photolysis experiments.

Cell culture

Human breast cancer cell line MCF-7 (ATCC, HTB-22) was cultured at 37 °C under a humidified atmosphere of 5% CO_2. The cells were grown in Eagle's Minimum Essential Medium (EMEM, ATCC, 30-2003) supplemented with 10% fetal bovine serum (Gibco, 10437028), 1% antibiotics (100 U/mL penicillin and 100 µg/mL streptomycin, Gibco, 105140122), and 10 µg/mL bovine insulin (Sigma, I0516). The cells were continuously maintained in the culture medium and subcultured every 3–4 days.

Drug treatment and cell viability assay

MCF-7 cells were seeded at 10,000 cells/well in a 96-well plate and allowed to attach for 20 h before drug treatment. Prior to drug exposure, the culture medium was removed and the cells were washed once with warm phosphate-buffered saline (PBS). Then, fresh media with drug concentrations ranging from 0 to 100 µM (based on dry weight of polymer dissolved in H_2O) were added to the appropriate wells. After recovering for 10 min at 37 °C, one plate of cells was submitted to UV light (Multiple Ray Lamp with filtered blacklight bulb, 365 nm) for 10 min while the control plate was kept in the dark. The cells were subsequently incubated in a cell culture incubator for 24 h. The medium was removed and the cells were washed twice with warm PBS before fresh drug-free medium was added to each well. The cells were incubated for another 24 h before analysis by the MTT cell proliferation assay (ATCC, 30-1010K). Cells were washed once with warm PBS and incubated with fresh medium containing MTT reagent for 3 h at 37 °C. Detergent was added to solubilize the purple formazan crystals formed by proliferating cells. Absorbance at 570 nm was measured on a Safire II (Tecan) plate reader. Data were fit to a sigmoidal function to determine the half-maximum inhibitory concentration (IC_{50}).

Results and Discussion

Synthesis of norbornene-PEG-alkyne MM

Graft-through ROMP reduces the problem of brush polymer synthesis to design of an appropriate, strained alkene MM; a bivalent-brush is derived from a bivalent norbornene MM (Figure 1). Using a branched MM avoids the need for copolymerization of two different monomers, one PEG-MM and one drug-loaded monomer; a high drug loading is maintained and issues arising from different propagation rates between MM and small-molecule monomers are negated. Toward this end, we prepared norbornene-imide derivative **6** (Schemes 1 and 4) which carries two orthogonally addressable functional groups, an *N*-hydroxysuccinimidyl (NHS) ester and an alkyne. The NHS-ester of **6** was efficiently coupled to water soluble PEG-NH$_2$ (M_n = 3 kDa) to give PEG-MM **7** (Figure 2). We independently prepared **DOX**- and **CT**- nitrobenzyloxycarbonyl-azide analogues (**DOX-NBOC-N$_3$** and **CT-NBOC-N$_3$**, Scheme 2 and Figure 2) that allow for drug attachment via copper-catalyzed azide-alkyne cycloaddition (CuAAC) click chemistry[48−50] and controlled drug release in response to long wavelength UV irradiation (~365 nm). CuAAC coupling of **3** to either drug-azide proceeded in high yield to give the desired drug-loaded PEG-MMs (**DOX-MM** and **CT-MM**). The MALDI spectra of **CT-MM** and its alkyne precursor **7** confirmed the expected mass increase after CuAAC coupling (Figure 2).

ROMP of drug-loaded, PEGylated MMs

Treatment of either MM with **1** in methylene chloride (DCM) for 90 min under N$_2$ yielded polymers (**pDOX** and **pCT**) with low PDIs and M_n dependent on the ratio of MM to **1** (Table I). The **pDOX** brushes were characterized by PDIs on the order of 1.1 as previously reported for graft-through ROMP polymerizations using catalyst **1**.[27,28] The PDI values for **pCT** samples were low for DP$_n$ below ~30 but higher at high DP$_n$ and the overall attainable DP$_n$ was limited to ~150. For *in vivo* delivery of non-degradable polymers, hydrodynamic radii of $< 5 – 10$ nm are often desirable[35,42]; graft-through ROMP of either MM is highly controlled within this size domain (Table I). For the higher DP$_n$ **CT-MM** polymerizations, we hypothesize that the presence of potential chelating moieties (quinoline and pyrrole) in **CT** may interfere with catalyst initiation and propagation especially at high DP$_n$. Nevertheless, the success of the graft-through ROMP polymerizations for both MMs attests to the remarkable functional-group tolerance of catalyst **1**. Figure 2 shows gel-permeation chromatography (GPC) traces of brush polymer samples **pCT03** and **pDOX02** without purification, confirming a mono-modal MW distribution and a very high conversion (>95%). All of the polymer samples were highly soluble in water (>100 mg / mL); trace MM was removed by passage of an aqueous solution of polymer through a 30 kDa cut-off centrifuge filter to give pure brush polymer (Figure 3, red trace). The purified samples were lyophilized to dryness and re-dissolved in water prior to subsequent experiments.

As demonstrated above, graft-through ROMP allows for rapid access to brush polymers of controlled, variable molecular weights. We envisioned this methodology also being useful for preparing multiple-drug-loaded brush polymers via copolymerization of appropriate MMs. For example, treatment of equimolar mixtures of **DOX-MM** and **CT-MM** with catalyst **1** in DCM yielded copolymer **pDOX$_{50}$-pCT$_{50}$** which exhibited a narrow, monomodal MW distribution (Table I, Figure 3). Combination of a variety of therapeutic moieties within the same polymer system and controlled release using external, and perhaps different, stimuli will enable study and discovery of synergistic drug effects and design of synchronized drug releasing systems.

UV photolysis experiments

To demonstrate controlled release of **DOX** and **CT** from these brush polymer scaffolds in response to 365 nm UV light we irradiated aqueous solutions of the polymers for various times from 30 s to 10 min and monitored the progress of photorelease by high-performance liquid chromatography connected in series to a single wavelength UV detector and an electrospray mass spectrometer (LC-MS). The resulting chromatograms for brush polymer **pDOX02** (~1.1 µM of bound **DOX** in H_2O) before and after irradiation are shown in Figure 4a. With increasing irradiation time, the polymer absorbance at 500 nm is diminished and a new peak is observed at ~3.1 min; the mass of the species giving rise to this new peak is 542.30 Da which corresponds to that of free **DOX** - H^+. The yield for photocleavage in this time was ~50% based on integration of the polymer and free **DOX** peaks.

Similar data for **pCT03** (~2.6 µM bound **CT** in H_2O) are shown in Figure 4b. After 10 min irradiation we observed ~64% release of free **CT** along with two minor peaks labelled "*" in Figure 4b. **CT** is a common target for drug delivery because it is highly active against cancer cells but insoluble and unstable in neutral, aqueous solution.[47] We believe that these two peaks may represent degradation products of **CT** that result from hydrolysis (open lactone form) or photochemical degradation; however we have been unable to generate the same chromatogram by simply photolyzing free **CT** in solution due to its insolubility and we did not observe a molecular ion in the LC-MS that corresponds to the mass of the open lactone form (the major peak at ~4.1 min corresponds to the therapeutically-active lactone form of **CT**). These experiments show that the **pCT** brush polymers effectively solubilize their **CT** payload and allow for drug release even in aqueous solution where the **CT** cargo is insoluble.

We recorded the UV-Vis absorption spectra for **pDOX01**, **pCT01**, and **pDOX$_{50}$-pCT$_{50}$** in water to verify that **CT** and **DOX** were present (Figure 5a). The spectra of **pCT01** and **pDOX01** display broad absorption bands at wavelengths above 300 nm that result from bound **CT** or **DOX**, respectively. The spectrum of the copolymer shows both bands. This information, along with the monomodal GPC trace (Figure 3) and photolysis data (Figure 5b) suggests that copolymer **pDOX$_{50}$-pCT$_{50}$** does indeed carry both drug molecules bound to the same polymer chain (rather than a mixture of two homopolymers which would likely result in broadening of the GPC trace). HPLC traces for the copolymer (~1.5 µM in H_2O) both before and after irradiation are shown in Figure 5b. Absorption was monitored at two wavelengths, 368 nm and 500 nm, to detect **CT** and **DOX** respectively. As expected, UV irradiation induced release of both drugs from the copolymer; to our knowledge this is the first example of a polymer system capable of releasing two covalently bound anti-cancer drugs (**DOX** and **CT**) in response to a controlled external stimulus. A recent report by Shen and coworkers suggests that materials capable of releasing both **DOX** and **CT** will display synergistic cytotoxicity when compared to either drug alone.[51]

Cell culture studies

To confirm that these drug-bound, PEG-based brush polymers were inherently non-toxic, and that photo-initiated drug release did indeed yield sufficient amounts of chemotherapeutic agent to kill cancer cells, we performed cell viability experiments using MCF-7 human breast cancer cells. Cells were treated with aqueous solutions of either free drug or the corresponding drug-loaded brush polymer at various concentrations and irradiated for 10 min using 365 nm light or kept in the dark. The cells were then incubated in the dark for 24 h, washed twice, and incubated for another 24 h in fresh, drug-free growth medium. After this time, cell viability was assessed using the MTT assay (see methods and materials for details). Representative data are shown in Figures 6a, 6b, and 6c. In Figures 6a and 6b both free **CT** and **DOX** controls, with and without UV irradiation, gave similar dose-

response curves with IC_{50} values of ~1.2 µM and ~4.9 µM, respectively. These data suggest that UV irradiation at 365 nm for 10 min is not by itself toxic to the cells nor is it detrimental to the drug toxicity. On the other hand, polymer samples **pCT01** and **pDOX02** without UV irradiation were non-toxic to cells at concentrations greater than 10 times those of the free drugs (39 µM and 105 µM, respectively) indicating that the PEG brush polymers effectively shield the toxic effects of **CT** and **DOX** prior to drug release. We were pleased to find that irradiation of the drug-bound polymers led to greatly increased cytotoxicity (IC_{50} = 2.2 µM and 8.7 µM for **pCT01** and **pDOX02**, respectively) compared to the non-irradiated samples suggesting that photoreleased **CT** and **DOX** were therapeutically effective. Figure 6c compares the toxicity of copolymer **pDOX$_{50}$-pCT$_{50}$** with a 1:1 mixture of **pDOX02** and **pCT01** before and after irradiation. The copolymer was non-toxic prior to irradiation at concentrations less than 100 µM whereas the mixture of both polymers appeared to be toxic at lower concentration (29 µM). UV induced drug release, however, led to a similar IC_{50} for both systems (3.2 µM for **pDOX$_{50}$-pCT$_{50}$** and 2.2 µM for the mixture). Figure 6d shows the therapeutic factors (*X*) for these materials: a measure of the increase in cytotoxicity after photo-induced drug release. All of the polymers studied showed at least a 12X increase in toxicity upon drug release; these results are encouraging and suggest the utility of these brush polymer systems for *in vivo* drug delivery applications.

Conclusions

To our knowledge this report is the first example of simultaneous photo-regulated release of **DOX** and **CT** and the first example of bivalent-brush polymers capable of controlled release of anticancer drugs (for other examples of photorelease of anticancer drugs see52−54). The graft-through approach ensures that the weight percentage of drug loaded onto the brush polymers is the same as the weight percentage of drug on the MM (because of 100% grafting density) and is independent of DP_n and conversion. Thus, **pCT** and **pDOX** polymers carry 8.5% **CT** and 12.6% **DOX** by weight, respectively. These values could be increased by shortening the length of the PEG sidechain prior to ROMP or designing an MM linked to more than one drug molecule. The synthesis of these materials was facilitated by the graft-through ROMP paradigm and we expect this approach to prove useful for the synthesis of a range of other functional multivalent-brush polymer systems. We are also developing clickable linkers with alternate drug release mechanisms; one limitation of this system is the requirement for UV light to initiate drug release. Though long-wavelength UV (UVA) is used for photochemotherapeutic treatment of various cancers and skin disorders, 55−61 there is need for new photocleavable groups with longer absorption wavelengths and high two-photon cross sections to increase tissue penetration.62,63 The modularity of this system combined with the versatility of graft-through ROMP will enable incorporation of new cleavable linkers into bivalent-brush polymers.

Supplementary Material

Refer to Web version on PubMed Central for supplementary material.

Acknowledgments

References

1. Hawker CJ, Wooley KL. Science (Washington, DC, U. S.). 2005; 309:1200–1205.

2. Hawker CJ, Fokin VV, Finn MG, Sharpless KB. Aust. J. Chem. 2007; 60:381–383.

3. Kolonko EM, Pontrello JK, Mangold SL, Kiessling LL. J. Am. Chem. Soc. 2009; 131:7327–7333. [PubMed: 19469577]

4. Conrad RM, Grubbs RH. Angew. Chem., Int. Ed. 2009; 48:8328–8330.

5. Clark PM, Dweck JF, Mason DE, Hart CR, Buck SB, Peters EC, Agnew BJ, Hsieh-Wilson LC. J. Am. Chem. Soc. 2008; 130:11576–11577. [PubMed: 18683930]

6. Rawat M, Gama CI, Matson JB, Hsieh-Wilson LC. J. Am. Chem. Soc. 2008; 130:2959–2961. [PubMed: 18275195]

7. Yuan Y-Y, Du Q, Wang Y-C, Wang J. Macromolecules. 2010; 43:1739–1746.

8. Li C, Ge Z, Fang J, Liu S. Macromolecules. 2009; 42:2916–2924.

9. Li A, Lu Z, Zhou Q, Qiu F, Yang Y. J. Polym. Sci., Part A Polym. Chem. 2006; 44:3942–3946.

10. Zhang M, Mueller AHE. J. Polym. Sci., Part A: Polym. Chem. 2005; 43:3461–3481.

11. Jiang X, Lok MC, Hennink WE. Bioconj. Chem. 2007; 18:2077–2084.

12. Tsarevsky NV, Bencherif SA, Matyjaszewski K. Macromolecules. 2007; 40:4439–4445.

13. Lutz J-F, Boerner HG, Weichenhan K. Macromolecules. 2006; 39:6376–6383.

14. Allen MJ, Wangkanont K, Raines RT, Kiessling LL. Macromolecules. 2009; 42:4023–4027. [PubMed: 20161406]

15. Cheng G, Boeker A, Zhang M, Krausch G, Mueller AHE. Macromolecules. 2001; 34:6883–6888.

16. Lu H, Wang J, Lin Y, Cheng J. J. Am. Chem. Soc. 2009; 131:13582–13583. [PubMed: 19725499]

17. Morandi G, Pascual S, Montembault V, Legoupy S, Delorme N, Fontaine L. Macromolecules. 2009; 42:6927–6931.

18. Neugebauer D, Sumerlin BS, Matyjaszewski K, Goodhart B, Sheiko SS. Polymer. 2004; 45:8173–8179.

19. Sumerlin BS, Neugebauer D, Matyjaszewski K. Macromolecules. 2005; 38:702–708.

20. Gao H, Matyjaszewski K. J. Am. Chem. Soc. 2007; 129:6633–6639. [PubMed: 17465551]

21. Hadjichristidis N, Pitsikalis M, Iatrou H, Pispas S. Macromol. Rapid Commun. 2003; 24:979–1013.

22. Tsukahara Y, Mizuno K, Segawa A, Yamashita Y. Macromolecules. 1989; 22:1546–1552.

23. Tsukahara Y, Tsutsumi K, Yamashita Y, Shimada S. Macromolecules. 1990; 23:5201–5208.

24. Dziezok P, Sheiko SS, Fischer K, Schmidt M, Moller M. Angew. Chem., Int. Ed. 1998; 36:2812–2815.

25. Neiser MW, Okuda J, Schmidt M. Macromolecules. 2003; 36:5437–5439.

26. Neiser MW, Muth S, Kolb U, Harris JR, Okuda J, Schmidt M. Angew. Chem., Int. Ed. 2004; 43:3192–3195.

27. Xia Y, Kornfield JA, Grubbs RH. Macromolecules. 2009; 42:3761–3766.

28. Xia Y, Olsen BD, Kornfield JA, Grubbs RH. J. Am. Chem. Soc. 2009; 131:18525–18532. [PubMed: 19947607]

29. Li Z, Zhang K, Ma J, Cheng C, Wooley KL. J. Polym. Sci., Part A: Polym. Chem. 2009; 47:5557–5563.

30. Li Z, Ma J, Cheng C, Zhang K, Wooley KL. Macromolecules. 2010; 43:1182–1184.

31. Le D, Montembault V, Soutif JC, Rutnakornpituk M, Fontaine L. Macromolecules. 2010; 43:5611–5617.

32. Duncan R. Nat. Rev. Drug Discovery. 2003; 2:347–360.

33. Peer D, Karp JM, Hong S, Farokhzad OC, Margalit R, Langer R. Nat. Nanotechnol. 2007; 2:751–760. [PubMed: 18654426]

34. Mammen M, Chio S-K, Whitesides GM. Angew. Chem., Int. Ed. 1998; 37:2755–2794.

35. Fox ME, Szoka FC, Frechet JMJ. Acc. Chem. Res. 2009; 42:1141–1151. [PubMed: 19555070]

36. Matsumura Y, Maeda H. Cancer Res. 1986; 46:6387–6392. [PubMed: 2946403]

37. Tomalia DA, Baker H, Dewald J, Hall M, Kallos G, Martin S, Roeck J, Ryder J, Smith P. Polym. J. (Tokyo, Jpn.). 1985; 17:117–132.

38. Bosman AW, Janssen HM, Meijer EW. Chem. Rev. (Washington, DC, U. S.). 1999; 99:1665–1688.

39. Lee CC, Gillies ER, Fox ME, Guillaudeu SJ, Frechet JMJ, Dy EE, Szoka FC. Proc. Natl. Acad. Sci. U. S. A. 2006; 103:16649–16654. [PubMed: 17075050]

40. Guillaudeu SJ, Fox ME, Haidar YM, Dy EE, Szoka FC, Frechet JMJ. Bioconj. Chem. 2008; 19:461–469.

41. Fox ME, Guillaudeu S, Frechet JMJ, Jerger K, Macaraeg N, Szoka FC. Mol. Pharm. 2009; 6:1562–1572. [PubMed: 19588994]

42. Grayson SM, Godbey WT. J. Drug Targeting. 2008; 16:329–356.

43. Love JA, Morgan JP, Trnka TM, Grubbs RH. Angew. Chem., Int. Ed. 2002; 41:4035–4037.

44. Vercillo OE, Andrade CKZ, Wessjohann LA. Org. Lett. 2008; 10:205–208. [PubMed: 18088132]

45. Johnson JA, Finn MG, Koberstein JT, Turro NJ. Macromolecules. 2007; 40:3589–3598.

46. Pangborn AB, Giardello MA, Grubbs RH, Rosen RK, Timmers FJ. Organometallics. 1996; 15:1518–1520.

47. Zhao H, Lee C, Sai P, Choe YH, Boro M, Pendri A, Guan S, Greenwald RB. J. Org. Chem. 2000; 65:4601–4606. [PubMed: 10959865]

48. Kolb HC, Finn MG, Sharpless KB. Angew. Chem., Int. Ed. 2001; 40:2004–2021.

49. Rostovtsev VV, Green LG, Fokin VV, Sharpless KB. Angew. Chem., Int. Ed. 2002; 41:2596–2599.

50. Tornoe CW, Christensen C, Meldal M. J. Org. Chem. 2002; 67:3057–3064. [PubMed: 11975567]

51. Shen Y, Jin E, Zhang B, Murphy CJ, Sui M, Zhao J, Wang J, Tang J, Fan M, Van Kirk E, Murdoch WJ. J. Am. Chem. Soc. 2010; 132:4259–4265. [PubMed: 20218672]

52. Agasti SS, Chompoosor A, You C-C, Ghosh P, Kim CK, Rotello VM. J. Am. Chem. Soc. 2009; 131:5728–5729. [PubMed: 19351115]

53. Kim H-C, Hartner S, Behe M, Behr Thomas M, Hampp Norbert A. J. Biomed. Opt. 2006; 11:34024. [PubMed: 16822073]

54. Choi SK, Thomas T, Li M-H, Kotlyar A, Desai A, Baker JR Jr. Chem. Commun. (Cambridge, U. K.). 2010; 46:2632–2634.

55. Krutmann J. J. Photochem. Photobiol., B. 1998; 44:159–164. [PubMed: 9757598]

56. Bethea D, Fullmer B, Syed S, Seltzer G, Tiano J, Rischko C, Gillespie L, Brown D, Gasparro FP. J. Dermatol. Sci. 1999; 19:78–88. [PubMed: 10098699]

57. Breuckmann F, Gambichler T, Altmeyer P, Kreuter A. BMC Dermatol. 2004; 4 No pp given.

58. Diffey B. Phys. Med. Biol. 2006; 51:R229–R244. [PubMed: 16790905]

59. Dolmans DEJGJ, Fukumura D, Jain RK. Nat. Rev. Cancer. 2003; 3:380–387. [PubMed: 12724736]

60. Dolmans DEJGJ, Kadambi A, Hill JS, Flores KR, Gerber JN, Walker JP, Borel Rinkes IHM, Jain RK, Fukumura D. Cancer Res. 2002; 62:4289–4294. [PubMed: 12154031]

61. Wozniak MB, Tracey L, Ortiz-Romero PL, Montes S, Alvarez M, Fraga J, Herrera JF, Vidal S, Rodriguez-Peralto JL, Piris MA, Villuendas R. Br. J. Dermatol. 2009; 160:92–102. [PubMed: 18945306]

62. Buckup T, Southan A, Kim HC, Hampp N, Motzkus M. J. Photochem. Photobiol., A. 2010; 210:188–192.

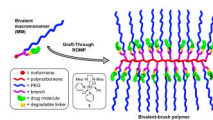63. Haertner S, Kim H-C, Hampp N. J. Polym. Sci., Part A Polym. Chem. 2007; 45:2443–2452.

Figure 1.
Schematic depiction of bivalent macromonomer (MM) and bivalent-brush polymer described in this work.
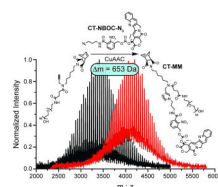
Figure 2.
MALDI spectra for PEG-norbornene **3** before (black trace) and after (red trace) CuAAC click coupling of **CT-NBOC-N₃** to give **CT-MM**. The observed mass shift of 653 Da agrees with the calculated mass of **CT-NBOC-N₃** and confirms successful attachment of the photocleavable drug moiety.
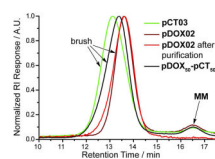
Figure 3.
Representative GPC traces for brush polymer samples. Black and red chromatograms correspond to crude ROMP reaction mixtures. The brush polymers display narrowly dispersed, mono-modal molecular weight distributions. The GPC trace for purified **pDOX02** is shown in orange, indicating that it is possible to remove trace MM impurity.
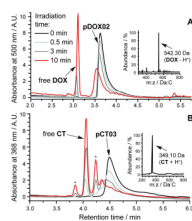
Figure 4.
HPLC-MS traces of aqueous brush polymer solutions before and after 365 nm UV irradiation for various times. **pDOX02** and **pCT03** yield free **DOX** and **CT**, respectively. LC-MS method A (see methods and materials) was used for **pDOX02** while method B was used for **pCT03**. Inset mass spectra, obtained from the free **DOX** and **CT** peaks, show strong signals at m:z ratios that correspond to the molecular ions of **DOX** and **CT**.
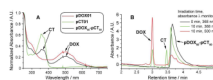
Figure 5.
A: UV-Vis absorption of **pDOX01**, **pCT01**, and copolymer **pDOX$_{50}$-pCT$_{50}$**. **B:** HPLC traces of an aqueous solution of **pDOX$_{50}$-pCT$_{50}$** before and after 365 nm UV irradiation for 10 min.
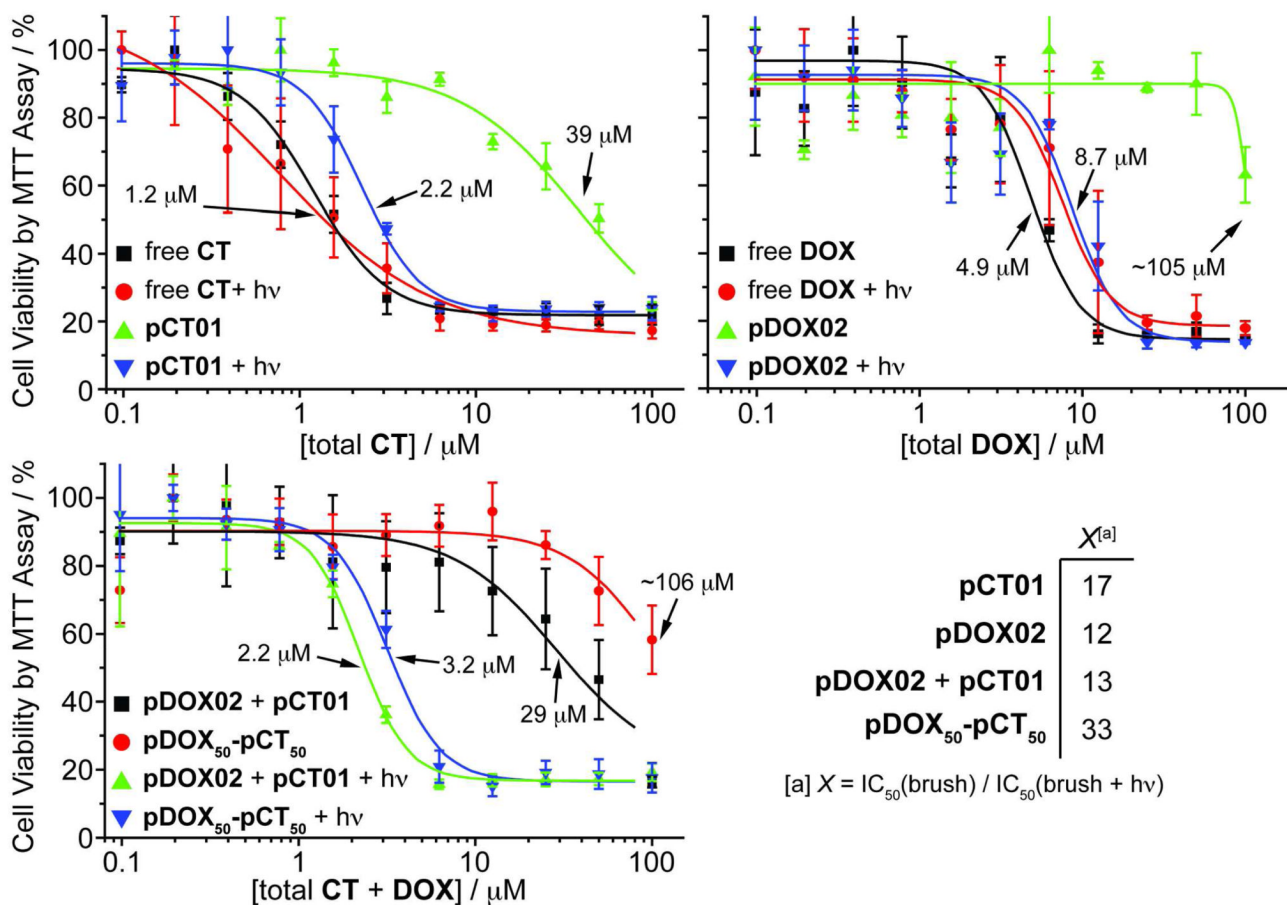
Figure 6.
A–C: Viability of MCF-7 human breast cancer cells treated with free **DOX** and **CT** and drug-loaded brush polymers both with and without UV irradiation. Data points were fit to a sigmoidal function and the half-maximum inhibitory concentrations (IC_{50}) are shown. The *x*-axis labels refer to the concentration of both free and polymer-conjugated drug. **D:** Table of therapeutic factors for each brush polymer formulation. These values represent the fold-increase in toxicity after irradiation and drug release.
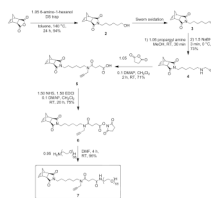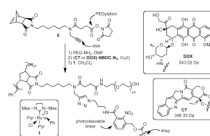
Scheme 1.
Synthesis of PEG-norbornene-alkyne macromonomer **3**.
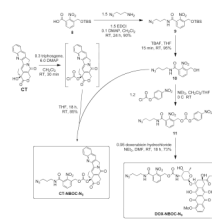
Scheme 2.
Synthesis of clickable, photocleavable drugs **CT-NBOC-N₃** and **DOX-NBOC-N₃**.
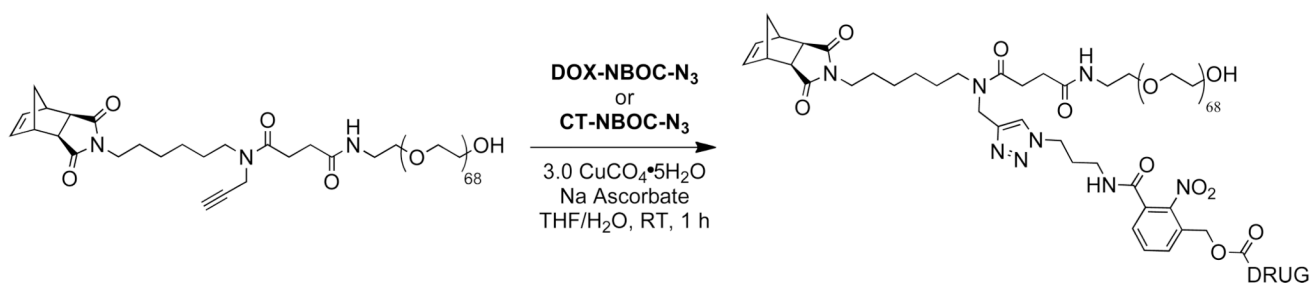
Scheme 3.
Click coupling of **3** to photocleavable drug derivatives.

Scheme 4.
Synthesis and structure of poly(norbornene)-PEG brush polymers with **DOX** or **CT** attached via a photocleavable NBOC linker.

Table I

GPC characterization of **pDOX** and **pCT** brush polymer samples and random copolymer **pDOX$_{50}$-pCT$_{50}$**.

sample	MM:1[a]	DP$_n$[b]	M$_n$ (GPC, kDa)	PDI	D$_h$[c]
pDOX01	10	9	33.7	1.07	6.2 (0.5)
pDOX02	50	58	227	1.05	12 (2)
pDOX03	100	96	352	1.04	15 (2)
pCT01	15	15	55.4	1.09	7.1 (0.5)
pCT02	25	30	111	1.17	8.7 (0.9)
pCT03	100	75	276	1.38	n.d.[e]
pCT04	150	107	394	1.61	n.d.
pCT05	200	135	499	1.70	n.d.
pDOX$_{50}$-pCT$_{50}$[d]	100	101	393	1.13	15 (1)

[a] ratio of MM to catalyst (i.e. theoretical DP$_n$),

[b] DP$_n$ observed derived from M$_n$(GPC) / M$_n$(MM),

[c] hydrodynamic diameter measured by dynamic light scattering (DLS) using the CONTIN fitting algorithm. Reported values are the average of three experiments with error shown in parentheses.

[d] **pDOX50-pCT50** carries approximately 50 **DOX** and 50 **CT** based on MM stoichiometry prior to ROMP,

[e] D$_h$ values not determined for these samples due to high polydispersity.